# Magnetic Properties and Phase Transitions in $(CH_3NH_2)K_3C_{60}$ Fulleride: An $^1H$ and $^2H$ NMR Spectroscopic Study

Denis Arčon,*[,†,‡] Alexey Y. Ganin,[§] Yasuhiro Takabayashi,[||] Matthew J. Rosseinsky,*[,§] and Kosmas Prassides*[,||]

*Insitute Jozef Stefan, Jamova 39, 1000 Ljubljana, Slovenia, Faculty of Mathematics and Physics, University of Ljubljana, Jadranska 19, 1000 Ljubljana, Slovenia, Department of Chemistry, University of Liverpool, Liverpool L69 7ZD, United Kingdom, and Department of Chemistry, University of Durham, Durham DH1 3LE, United Kingdom*

*Received February 28, 2008. Revised Manuscript Received April 28, 2008*

The hyperexpanded $(CH_3NH_2)K_3C_{60}$ fulleride and its perdeuterated analogue were investigated by $^1H$ and $^2H$ NMR spectroscopy between room temperature and 4 K. Two phase transitions at $T_S = 220$ K and $T_N = 11$ K clearly were detected in the temperature dependence of the NMR line shapes, the spectral first ($M_1$) and second ($M_2$) moments, and the spin lattice relaxation times, $T_1$. From $^2H$ NMR line shape analysis, we found that the structural phase transition at $T_S$ was driven by the freezing out of the discrete Markovian-type jump motion of the entire $K^+$-$ND_2CD_3$ unit that is characterized by an activation energy, $E_a = 236(51)$ meV. Below $T_S$, a sudden change in the temperature dependence of $M_1$ suggests the appearance of a small but nonzero spin density on the $K^+$-$NH_2CH_3$ unit. This could influence the electronic properties of the fulleride phase by modulating the strength of the exchange interactions between $C_{60}^{3-}$ anions and controlling the width, $W$, of the $t_{1u}$-derived band. The $^1H$ NMR spectra below $T_N$ show significant line broadening consistent with the onset of long-range antiferromagnetic order. $^1H$ NMR line shape calculations revealed the adoption of a type II magnetic structure with an ordering vector, $\vec{q}_{II} = (1/2, 1/2, 1/2)$ and individual $C_{60}^{3-}$ magnetic moments of magnitude ($\sim 0.7\ \mu_B$) aligned along the crystallographic $a$-axis.

## Introduction

The issues of metal−/superconductor−insulator transitions and strongly correlated physics in fullerides[1,2] have recently received new interest by the discovery of bulk superconductivity at 38 K—the highest $T_c$ known for any molecular material—for the cubic A15-structured $Cs_3C_{60}$ material.[3] Access to these compositions was provided by a solution-based route where $CH_3NH_2$ was employed to synthesize suitable methylaminated alkali fulleride precursors that were mildly heated to remove the cointercalated solvent. However, the precursors themselves are of significant interest as they also provide a route to hyperexpanded fullerides in which $C_{60}^{3-}$ electronic contact may be retained at very large interfullerene separations. Indeed, we have shown that cointercalation of $CH_3NH_2$ units into the octahedral voids of the cubic $K_3C_{60}$ fulleride lattice leads to a phase with stoichiometry $(CH_3NH_2)K_3C_{60}$ and a strongly anisotropic highly expanded face-centered orthorhombic unit cell (space group *Fmmm*).[4] The resulting unit cell volume per $C_{60}$, $V = 779.1$ Å$^3$, is one of the largest achieved thus far among alkali-doped fullerides. In addition, the expansion driven by the elongated $CH_3NH_2$ intercalant is very anisotropic with the shortest and longest distances between neighboring $C_{60}$ units of 10.163 and 10.742 Å, respectively. The structural expansion and accompanying anisotropy have important consequences in determining the electronic ground state of the $(CH_3NH_2)K_3C_{60}$ system. Extensive X-band EPR measurements[5] provided compelling evidence that $(CH_3NH_2)K_3C_{60}$ is nonmetallic at temperatures between 4 and 300 K. Moreover, the disappearance of the X-band EPR signal together with the detection of an antiferromagnetic resonance (AFMR) in high-field EPR[6] and the onset of spontaneous oscillations in zero-field (ZF) $\mu$SR experiments[7] below $T_N = 11$ K provided firm evidence that its low-temperature electronic ground state is that of an AFM insulator.

The previous results are consistent with the survival of significant electronic contact between the $C_{60}^{3-}$ units even at these large interfulleride spacings and place $(CH_3NH_2)K_3C_{60}$ just beyond the Mott−Hubbard metal−insulator boundary in

* Corresponding authors. E-mail: (D.A.) denis.arcon@ijs.si; (M.J.R.) M.J.Rosseinsky@liverpool.ac.uk; (K.P.) K.Prassides@durham.ac.uk.
† Institute Jozef Stefan.
‡ University of Ljubljana.
§ University of Liverpool.
|| University of Durham.

(1) Gunnarsson, O. *Alkali-Doped Fullerides*; World Scientific: Singapore, 2004.
(2) Capone, M.; Fabrizio, M.; Castellani, C.; Tosatti, E. *Science (Washington, DC, U.S.)* **2002**, *296*, 2364.
(3) Ganin, A. Y.; Takabayashi, Y.; Khimyak, Y. Z.; Margadonna, S.; Tamai, A.; Rosseinsky, M. J.; Prassides, K. *Nat. Mater.* **2008**, *7*, 367.
(4) Ganin, A. Y.; Takabayashi, Y.; Bridges, C. A.; Khimyak, Y. Z.; Margadonna, S.; Prassides, K.; Rosseinsky, M. J. *J. Am. Chem. Soc.* **2006**, *128*, 14784.
(5) Ganin, A. Y.; Takabayashi, Y.; Pregelj, M.; Zorko, A.; Arčon, D.; Rosseinsky, M. J.; Prassides, K. *Chem. Mater.* **2007**, *19*, 3177.
(6) Arčon, D.; Pregelj, M.; Zorko, A.; Ganin, A. Y.; Rosseinsky, M. J.; Takabayashi, Y.; Prassides, K.; van Tol, H.; Brunel, L.-C. *Phys. Rev. B: Condens. Matter Mater. Phys.* **2008**, *77*, 35104.
(7) Takabayashi, Y.; Ganin, A. Y.; Rosseinsky, M. J.; Prassides, K. *Chem. Commun. (Cambridge, U.K.)* **2007**, 870.

10.1021/cm800578e CCC: $40.75 
Published on Web 06/14/2008

the electronic phase diagram of $C_{60}^{3-}$ compounds.[8,9] However, there remain several issues related to the impact of the $CH_3NH_2$ intercalant on the electronic properties that are far from being well-understood in this system and call for additional investigations. Synchrotron X-ray diffraction has revealed the occurrence of a structural phase transition at around $T_S = 220$ K.[4,5] Interestingly, the structural changes appear also to influence sensitively the electronic structure as evidenced by the EPR spin susceptibility and line width anomalies in the same temperature interval.[5] Possible candidates to drive these effects include orientational ordering of the $C_{60}^{3-}$ and/or $CH_3NH_2$ units. In addition, in analogy with the ammoniated alkali fulleride analogues,[10] the large $CH_3NH_2$ groups are in close proximity to $C_{60}$ molecules allowing for the occurrence of nonclassical hydrogen bonding[11–13] contacts that would influence the propagation of exchange interactions. As a result, the splitting of the $t_{1u}$ orbitals would be affected, and a partial charge polarization may accumulate in the vicinity of the H−$C_{60}$ contacts. This is particularly relevant when we consider that the observed $T_N$ of $(CH_3NH_2)K_3C_{60}$ is drastically smaller than those of the related $(NH_3)K_{3-x}Rb_xC_{60}$ analogues at the same volume per $C_{60}$ unit.[14–16] Finally, while ZF-$\mu$SR and AFMR measurements on powder samples unambiguously established the low-temperature AFM ground state, they cannot provide information concerning the details of the long-range ordered magnetic structure.

To address these issues, we undertook a detailed temperature-dependent $^1$H and $^2$H NMR spectroscopic study of $(CH_3NH_2)K_3C_{60}$ and its perdeuterated analogue. The structural phase transition at $T_S = 220$ K was found to arise from the ordering of the $CH_3NH_2$ units and led to the development of fullerene···H−C interactions that may be responsible for the anomalous reduction of the exchange interactions between the $C_{60}^{3-}$ moments when compared to the ammoniated alkali fulleride analogues. Low-temperature $^1$H NMR line shape analysis was consistent with the adoption by $(CH_3NH_2)K_3C_{60}$ of an ordered antiferromagnetic structure of type II [magnetic ordering vector, $\vec{q}_{II} = (1/2, 1/2, 1/2)$].

## Experimental Procedures

The powdered $(CH_3NH_2)K_3C_{60}$ and $(CD_3ND_2)K_3C_{60}$ samples were prepared by the reaction of single phase $K_3C_{60}$ powder with $CH_3NH_2$ or $CD_3ND_2$ vapor, as described before.[4] Sample purity was confirmed by synchrotron X-ray powder diffraction measurements on beamline ID31 ($\lambda = 0.63782$ Å) at the European Synchrotron Radiation Facility (ESRF), Grenoble, France.

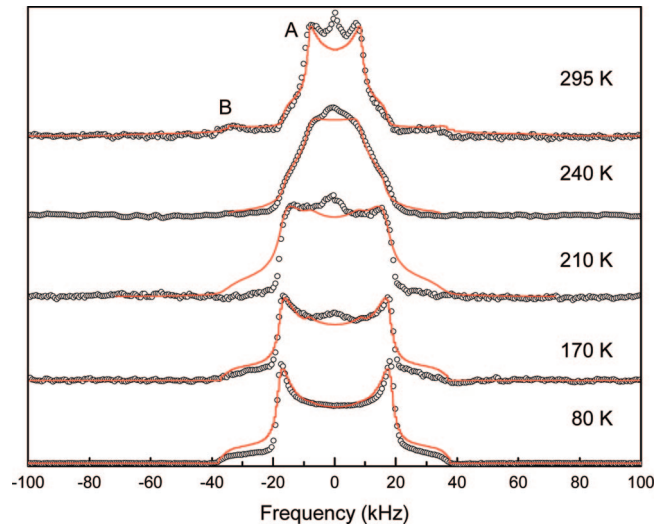


**Figure 1.** Temperature evolution of $^2$H NMR spectra measured for powdered $(CD_3ND_2)K_3C_{60}$. Solid lines represent fits to the model described in the text.

The $^1$H NMR spectra were recorded at a Larmor frequency, $\nu_L = 270$ MHz. A typical $\pi/2$ pulse length was 6 $\mu$s, which was not enough to excite the entire $^1$H NMR spectrum at low temperatures. For this reason, the frequency sweep technique with automatic tuning of the resonant circuit[17,18] was used below $T_N = 11$ K. The rf frequency was swept in 15 kHz steps, and the spectra were calculated as the integral of the signal as a function of the rf frequency. The $^2$H NMR spectra were measured at $\nu_L = 58.336$ MHz with a $\pi/2$ pulse length of 7 $\mu$s. In both experiments, an Oxford Instruments cryostat with a temperature stability better than ±0.1 K was used.

## Results

**Deuterium NMR Spectroscopy.** The deuterium ($I = 1$) NMR spectrum of the $(CD_3ND_2)K_3C_{60}$ polycrystalline sample at 295 K is dominated by a Pake-like quadrupolar powder line shape (Figure 1, labeled as A line) with the two main singularities at ±7.5(1) kHz and is suggestive of an axially symmetric electric field gradient tensor. Careful inspection of the spectra also reveals two additional peaks (Figure 1, labeled as B line) at ±35(1) kHz. In addition, a motionally narrowed component represented by a sharp peak at $\nu = 0$ also is evident. The temperature evolution of the NMR spectra at selected temperatures also is shown in Figure 1. Below 250 K, the NMR spectra begin to broaden with the line shape structure being gradually lost and the spectra progressively gaining in intensity at the high-frequency shoulders. At 220 K and below, a single quadrupolar powder line shape is recovered, but this time, the two main singularities are found at ±16.2(3) kHz. No additional components are evident. A small residual temperature dependence of the position of the two singularities can be seen down to ~160 K, where the final splitting is $\delta\nu = 35.4(6)$ kHz. No further changes in the line shape are observed to the lowest temperature of the present experiment

(8) Margadonna, S.; Prassides, K. *J. Solid State Chem.* **2002**, *168*, 639.
(9) Durand, P.; Darling, G. R.; Dubitsky, Y.; Zaopo, A.; Rosseinsky, M. J. *Nat. Mater.* **2003**, *2*, 605.
(10) Margadonna, S.; Prassides, K.; Shimoda, H.; Takenobu, T.; Iwasa, Y. *Phys. Rev. B: Condens. Matter Mater. Phys.* **2001**, *64*, 132414.
(11) Fowkes, A. J.; Fox, J. M.; Henry, P. F.; Heyes, S. J.; Rosseinsky, M. J. *J. Am. Chem. Soc.* **1997**, *119*, 10413.
(12) Margadonna, S.; Aslanis, E.; Prassides, K. *J. Am. Chem. Soc.* **2002**, *124*, 10146.
(13) Shiroka, T.; Fumera, G.; Ligabue, O.; Ricco, M.; Antonioli, G. C. *J. Chem. Phys.* **2006**, *124*, 204717.
(14) Prassides, K.; Margadonna, S.; Arčon, D.; Lappas, A.; Shimoda, H.; Iwasa, Y. *J. Am. Chem. Soc.* **1999**, *121*, 11227.
(15) Takenobu, T.; Muro, T.; Iwasa, Y.; Mitani, T. *Phys. Rev. Lett.* **2000**, *85*, 381.
(16) Arvanitidis, J.; Papagelis, K.; Takabayashi, Y.; Takenobu, T.; Iwasa, Y.; Rosseinsky, M. J.; Prassides, K. *J. Phys.: Condens. Matter* **2007**, *19*, 386235.
(17) Jeglič, P.; Blinc, R.; Apih, T.; Omerzu, A.; Arčon, D. *Phys. Rev. B: Condens. Matter Mater. Phys.* **2003**, *68*, 184422.
(18) Arčon, D.; Dolinsek, J.; Blinc, R.; Pokhodnia, K.; Omerzu, A.; Mihailovič, D.; Venturini, P. *Phys. Rev. B: Condens. Matter Mater. Phys.* **1996**, *53*, 14028.

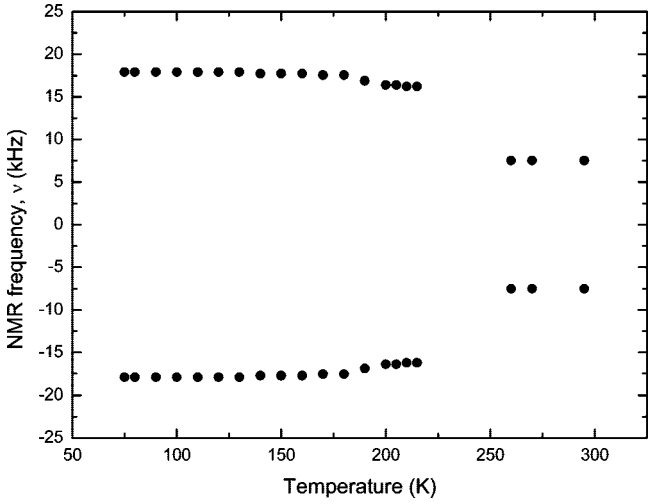


**Figure 2.** Temperature dependence of the two singularities in $^2$H NMR quadrupolar powder line shapes in $(CD_3ND_2)K_3C_{60}$.

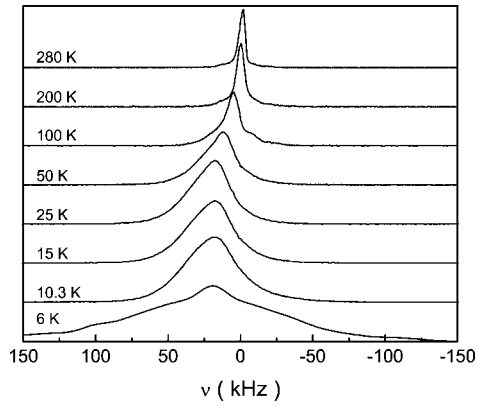


**Figure 3.** $^1$H NMR spectra measured at selected temperatures for powdered $(CH_3NH_2)K_3C_{60}$.

(70 K). Figure 2 shows the temperature dependence of the positions of the main singularities for line A. The observed behavior with changing temperature provides a clear signature of freezing out of the $CD_3ND_2$ dynamics across the structural phase transition in the vicinity of 220−230 K.

**$^1$H NMR Spectroscopy.** Although $^2$H NMR is very sensitive to structural phase transitions and molecular dynamics, it is a less suitable probe for the measurements of magnetic properties of a sample as the strong quadrupolar interactions typically dominate those between $^2$H nuclei and neighboring unpaired electrons. For this reason, we performed complementary temperature-dependent $^1$H NMR measurements on $(CH_3NH_2)K_3C_{60}$. Figure 3 shows the evolution of the $^1$H NMR spectra between room temperature and 6 K. The $^1$H NMR line shape exhibits a very complex behavior with change in temperature. The structural phase transition at ∼220 K is again sensed by (i) the broadening of the $^1$H NMR line, (ii) a gradual development of the line shape anisotropy, and (iii) the onset of a paramagnetic shift in the peak position. To quantify the changes in the $^1$H NMR spectra, we undertook moment analysis over the entire temperature range (Figure 4). Across the structural phase transition at 220 K, the square root of the second moment suddenly jumps from $\sqrt{M_2} = 2.9(1)$ kHz at 270 K to $\sqrt{M_2} = 4.5(2)$ kHz at 200 K. Below 200 K, $\sqrt{M_2}$ monotonically

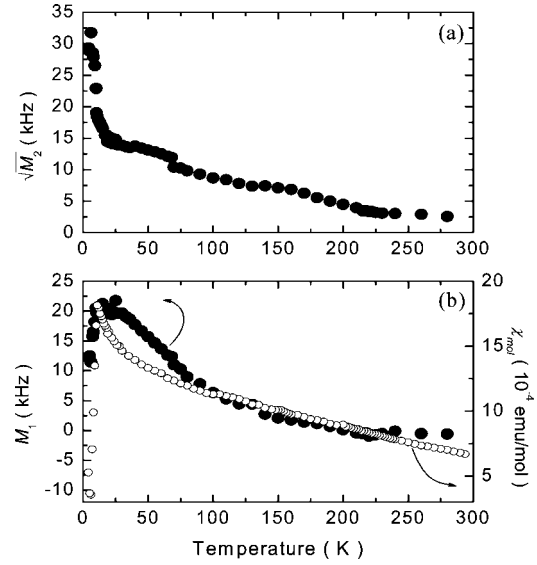


**Figure 4.** Temperature dependence of (a) the square root of the second moment, $\sqrt{M_2}$, and (b) the first moment, $M_1$, of the $^1$H NMR spectra in $(CH_3NH_2)K_3C_{60}$. In panel b, the temperature dependence of the X-band EPR spin susceptibility, $\chi_{mol}$, is also included for comparison.[5]

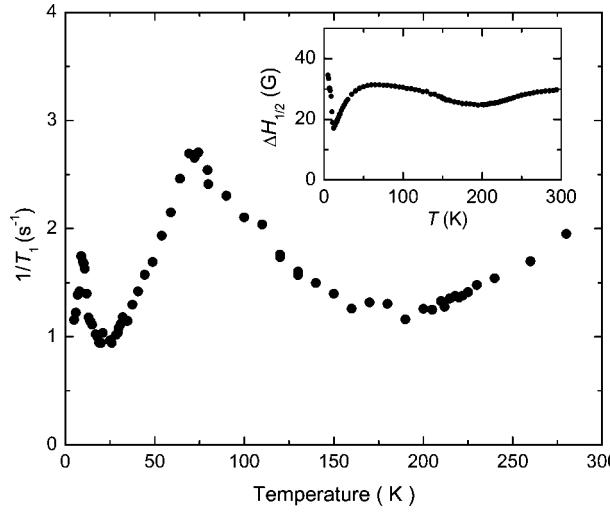


**Figure 5.** Temperature dependence of $^1$H NMR spin lattice relaxation rate, $1/T_1$. Inset: temperature dependence of the X-band EPR linewidth[5] shown for comparison.

increases with decreasing temperature (Figure 4a). As the temperature is lowered further below 100 K, the structure of the line shape fades away as the broadening continuously increases, until below 50 K we find a single asymmetric line shape. In addition to the pronounced broadening upon cooling, the paramagnetic shift of the spectra continues down to $T_N = 11$ K, where the shift of the first moment, $M_1$, from the reference frequency amounts to 80 ppm (Figure 4b). In the AFM phase, the shift is sharply reduced to 51 ppm at 4 K due to the reduction of the local field detected by the $^1$H nuclei. The transition to the AFM phase below 11 K is also signaled by additional broadening with $\sqrt{M_2}$ also sharply increasing to 32(2) kHz at 6 K.

We also note at this stage that a surprising feature of the $^1$H NMR data is that the structural phase transition is apparent in the temperature dependence of the first moment. Between room temperature and $T_S$, $M_1$ is nearly temperature independent. Following a small inflection at $T_S$, it is evident that

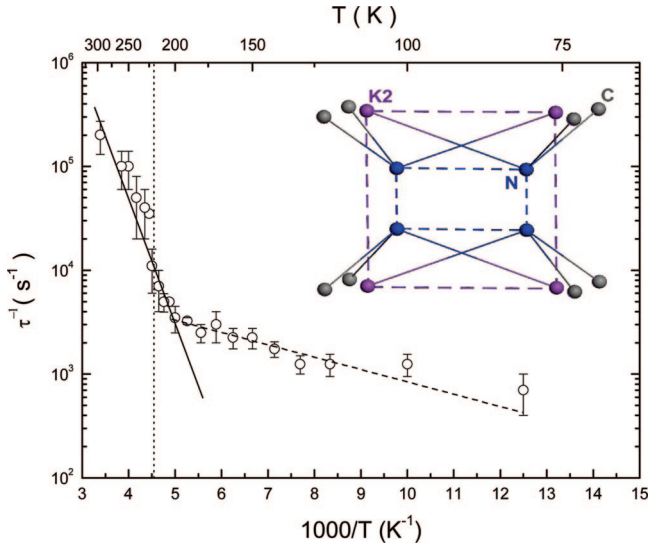


**Figure 6.** Temperature dependence of the $CD_3ND_2$ jump rate, $\tau^{-1}$, for reorientation of the K-N-C unit among the four available symmetry equivalent sites (inset). The solid line represents a fit to a high-temperature thermally activated type of motion with an activation energy, $E_a = 236(51)$ meV, while the dashed line is a fit to a low-temperature motion with activation energy, $E_a = 23(7)$ meV. The dotted vertical line marks the structural phase transition temperature at 220 K.

$M_1$ tracks the X-band EPR spin susceptibility, $\chi_{mol}$, down to ~75 K, where it begins to increase at a faster rate.

The observed changes in the $^1$H NMR spectra are accompanied by a very complex behavior of the temperature dependence of the spin lattice relaxation rate, $1/T_1$ (Figure 5). $1/T_1$ varies linearly upon cooling below 295 K toward $T_S$ and reaches a shallow minimum of 1.2 $s^{-1}$ at 200 K. Below 170 K, $1/T_1$ increases until it reaches a sharp maximum of 2.7 $s^{-1}$ at 70 K. Upon further cooling, the trend is reversed, and $1/T_1$ rapidly decreases again toward a minimum value of 0.9 $s^{-1}$, just above the Néel temperature. This is followed by a significant enhancement at $T_N$. Below $T_N$, the opening of the gap in the magnon spectrum is reflected in the suppression of the $1/T_1$ relaxation rate.

## Discussion

The $^2$H NMR technique is an established probe for the study of molecular dynamics in solids.[13,19–22] It has been used extensively through powder line shape analysis to characterize the mode of molecular motion and extract the relevant correlation times. At room temperature, $(CH_3NH_2)$-$K_3C_{60}$ adopts a face-centered orthorhombic structure in which the $CH_3NH_2$ units coordinate to the $K^+$ ions residing in the octahedral interstices of the unit cell, while uncoordinated $K^+$ ions occupy the tetrahedral holes. The $K^+$-$NH_2CH_3$ units are disordered over the corners of two concentric rectangles (inset in Figure 6).[4] The motional modes for the $CH_3NH_2$ molecules therefore involve most likely (i) rapid $CH_3$ rotations around the $C_3$ molecular axis, (ii) flipping of the $CH_3$ group from the site above to the site below the mirror plane, and finally (iii) random nearly 90° jumping of the entire $K^+$-$CH_3NH_2$ unit between the four available orientations. The present $^2$H NMR spectra with typical axially symmetric quadrupolar line shapes rule out a completely isotropic rotational diffusion motion of the $CD_3ND_2$ units but are consistent with a discrete Markovian jump mode of motion. In addition, the presence of two spectral components A and B at room temperature reflects the two inequivalent deuteron sites in the $CD_3ND_2$ molecule. Their assignment—$CD_3$ (A) and $ND_2$ (B)—is based on literature values for the quadrupole frequencies of $ND_2$ and $CD_3$ in $CD_3ND_2$ of ~290 and 40 kHz, respectively.[23] However, the reduced effective quadrupolar frequencies, $\nu_{QA} = 4/3\delta\nu_A = 20$ kHz and $\nu_{QB} = 4/3\delta\nu_B = 93.3$ kHz, at room temperature imply that the jump rate for the $CD_3ND_2$ units is fast on the NMR time scale. To simulate the $^2$H NMR spectra, we adopted a simplified model of $CD_3ND_2$ motion assuming that the $CD_3$ rotations around the $C_3$ molecular axis and the flipping of the N−C bond are both fast on the $^2$H NMR time scale (i.e., a typical jump rate for these motional modes is $\tau^{-1} \gg 10^6$ $s^{-1}$). Therefore, in our calculations, the $^2$H NMR line shape is affected only by nearly 90° random jumps of the entire $K^+$-$CD_3ND_2$ unit between the four available sites shown in the inset of Figure 6. Jumping between these sites is characterized by a single correlation rate, $\tau^{-1}$. These assumptions should be valid at least at high temperatures. The calculated room temperature $^2$H NMR spectrum is in excellent agreement with that measured experimentally (solid line in Figure 1) for a correlation rate of the jump motion, $\tau^{-1} \geq 200$ kHz. In the simulation, the contributions of the A and B components are taken to be in the ratio of 3:2 to reflect the appropriate number of D atoms in $CD_3ND_2$. However, the model is not capable of reproducing the narrow peak at the spectral center (Figure 1), which is a signature of isotropically reorienting molecules. This may thus reflect either the presence of a small fraction of uncoordinated $CD_3ND_2$ or alternatively that the time constant of the flipping of the N−C bond above and below the mirror plane also falls in the experimental time window.

Upon cooling, the motion of the $K^+$-$CD_3ND_2$ unit begins to slow. The $ND_2$ resonance broadens significantly, and it becomes difficult to detect it in our experiment. However, the changes in the $CD_3$ resonance allow for the extraction of the temperature dependence of the $K^+$-$CD_3ND_2$ jump rate (Figure 6) from the $^2$H NMR line shape simulation (solid lines in Figure 1). In the 290−80 K temperature interval, the jumping rates fall in the frequency window between $10^3$ and $10^6$ Hz. Clearly, two different motional regimes are evident, as at the structural phase transition temperature, $T_S = 220$ K, the correlation rate suddenly decreases by a factor of 5—from $\tau^{-1} = 35$ kHz at 225 K to $\tau^{-1} = 7$ kHz at 215 K. The motional dynamics in the high-temperature phase are characterized by an activation energy, $E_a = 236(51)$ meV. This value is much higher than that extracted for the motion of $NH_3$ groups in the related fulleride, $(NH_3)_xNaK_2C_{60}$ ($E_a$

(19) Mehring, M. *Principles of High Resolution NMR in Solids*; Springer: Berlin, 1983.
(20) Greenfield, M. S.; Ronemus, A. D.; Vold, R. L.; Ellis, P. D.; Raidy, T. E. *J. Magn. Reson.* **1987**, *72*, 89.
(21) Wittebort, R. J.; Olejniczak, E. T.; Griffin, R. G. *J. Chem. Phys.* **1987**, *86*, 5411.
(22) Tomaselli, M.; Meier, B. H. *J. Chem. Phys.* **2001**, *115*, 11017.
(23) Das, T. P.; Hahn, E. L. *Solid State Physics, Supplement 1: Nuclear Quadrupole Resonance Spectroscopy*; Academic Press: San Diego, 1958.

= 16 meV)[13] and is consistent with the larger and more anisotropic shape of the $K^+$-$CD_3ND_2$ unit. On the other hand, below 220 K, the low-temperature phase shows a nearly static powder spectrum characterized by very small jump rates. The remaining temperature dependence of the $^2H$ NMR line shape probably reflects the slowing of the motional modes that were neglected in our calculations. Since rotations of the $CD_3$ group around the $C_3$ axis are expected to freeze only at very low temperatures, we suggest that it is the flipping of the N-$CD_3$ axis that gradually slows on the $^2H$ NMR time scale below 220 K. Alternatively, small angle $ND_2$-$CD_3$ librations also could account for such behavior. Both motional modes can explain the slight reduction in the signal intensity at the center of the $^2H$ NMR spectra that is reflected in the line shape simulations as a very weak temperature dependence of $\tau$ and an extracted value of the low-temperature activation energy, $E_a = 23(7)$ meV. Such a small value of $E_a$ further corroborates the assumption of less restricted motion. In any case, the simulations of the $^2H$ NMR spectra even with the present simplified model clearly indicate that the structural phase transition observed in the XRD experiments is driven by the orientational ordering of the entire $K^+$-$CD_3ND_2$ unit. Such a scenario implies long-range ordering of the $K^+$-$CD_3ND_2$ electric dipole moments below 220 K, although the type of ordering (antiferroelectric vs ferroelectric) cannot be determined from the present data alone.

The dominance of the quadrupolar interactions in $^2H$ NMR experiments makes this probe less suitable to study the magnetic properties. For this reason, we now turn our attention to the $^1H$ NMR results. The appropriate spin Hamiltonian for $^1H$ ($I = 1/2$) can be written as

$$H = H_Z + H_{en} \tag{1}$$

where $H_Z = -\gamma_n \vec{\mathbf{I}} \vec{\mathbf{B}}_0$ is the Zeeman term, $H_{en} = \sum_i \vec{\mathbf{S}}_i \mathbf{A}_i \vec{\mathbf{I}}$ is the hyperfine coupling between nuclear, $\vec{\mathbf{I}}$, and neighboring $C_{60}^{3-}$ unpaired electronic, $\vec{\mathbf{S}}_i$ spins,[18,24] $\gamma_n$ and $\mathbf{A}_i$ are the nuclear gyromagnetic ratio and the electron−nuclear hyperfine tensor, respectively, and the sum goes over all neighboring $C_{60}^{3-}$ sites. The relevant information in our case is contained in the second term of eq 1 that can be further decomposed into an isotropic (Fermi contact) interaction, $H_{hf} = \sum a_i \vec{\mathbf{I}} \vec{\mathbf{S}}_i$ and an electron−nuclear dipolar interaction, $H_d = \sum_i \vec{\mathbf{S}}_i \mathbf{T}_i \vec{\mathbf{I}}$ term. The shift (or the first moment) of the $^1H$ resonance is given by the first term only since the dipolar tensor, $\mathbf{T}_i = \mu_0/4\pi(\gamma_n g \mu_B) \otimes (3\vec{\mathbf{n}}_i \otimes \vec{\mathbf{n}}_i - \mathbf{1})/r_i^3$ is traceless. Here, $\vec{\mathbf{n}}_i$ is the unit vector along the direction between the $^1H$ nucleus and the electron and $r_i$ is the $^1H$−electron distance. As the electronic spin dynamics are expected to be much faster than the NMR time scale at least in the paramagnetic phase, we can replace the electronic spin operator by its average value $\langle \vec{\mathbf{S}}_i \rangle$, which in turn in the paramagnetic phase is directly related to the molar spin susceptibility, $\langle \mathbf{S}_i \rangle = \chi_{mol} B_0 / 2 N_A g \mu_B$. The shift in the $^1H$ resonance, $\delta\nu$, depends on the magnitude of (i) the hyperfine contact constant, $a_i$, which is directly proportional to the electron spin density at the nuclear site, $\rho_S(0)$, and (ii) the spin susceptibility, $\chi_{mol}$, which can be measured for instance by EPR spectroscopy. In powder samples, one can thus express the shift of the resonance line as

$$\delta\nu = \frac{3 a_i}{h N_A g \mu_B} \chi_{mol} B_0 \tag{2}$$

On the other hand, the dipolar interactions participate only in the broadening of the NMR spectra, as discussed next.

Let us now return to the $^1H$ NMR results for $(CH_3NH_2)K_3C_{60}$. A key experimental finding is that the shift of the $^1H$ NMR spectra given by the first moment $M_1$ is very small and nearly temperature independent above $T_S$ but becomes suddenly temperature dependent below $T_S$ (Figure 4b). Moreover, $M_1$ tracks closely the spin susceptibility, $\chi_{mol}$, determined by the X-band EPR technique[5] in the temperature range between 220 and 70 K. To account for the change in $M_1$ at $T_S$, we need to postulate that the hyperfine contact constant, $a_i$, is temperature dependent (i.e., $a_i = 0$ for $T > T_S$ and $a_i \neq 0$ for $T < T_S$). Using eq 2, we can estimate that $a_i = 5(1) \times 10^{-6}$ cm$^{-1}$ at 150 K. The sudden increase in $a_i$, and therefore also in $\rho_S(0)$, below $T_S$ indicates that the structural transition is accompanied by the transfer of a very small unpaired spin charge density to the $CH_3NH_2$ molecule of the $K^+$-$NH_2CH_3$ unit. Combining this result with the conclusions drawn by the $^2H$ NMR spectral analysis, we find that the weak interaction between $C_{60}$ and $CH_3NH_2$ molecules appears only when the dynamics of the $K^+$-$NH_2CH_3$ units essentially completely freeze out. The small charge redistribution revealed by the NMR data below $T_S$ also can explain the accompanying gradual change in the electronic $g$-factor as observed by EPR.[5] However, we stress that the unpaired spin density at the $K^+$-$NH_2CH_3$ units is very small, at least in comparison to that in the ferromagnetic TDAE-$C_{60}$ fulleride where $^1H$ NMR shifts up to 370 ppm were measured.[21,22] Nevertheless, the observed temperature dependence of $M_1$ suggests the development of well-defined static fullerene···H−C interactions below $T_S$ in $(CH_3NH_2)$-$K_3C_{60}$ that are absent in the high-temperature disordered structure—also consistent with the unusually short C($C_{60}$)···H−C contacts of 2.25−2.32 Å observed crystallographically.[4] These effects should influence the electronic properties of the fulleride phase by modulating the strength of the exchange interactions between the $C_{60}^{3-}$ anions and the controlling the width, $W$, of the $t_{1u}$-derived band.

For temperatures below ~70 K, $M_1$ increases faster than $\chi_{mol}$ as the temperature decreases. This can be understood by recalling that $\chi_{mol}$ was determined by the integration of the X-band EPR spectra measured in a field of 0.34 T, while the $^1H$ NMR spectra were obtained at 6.3 T. The significant increase of $\langle \mathbf{S}_i \rangle$ at the higher magnetic field is presumably a signature of short-range magnetic effects, which become more pronounced with increasing magnetic field strength. However, these effects persist to unusually high temperatures, a situation typically encountered when the magnetic structure is of low dimensionality. Therefore, although the long-range magnetic order is three-dimensional below $T_N = 11$ K, low-dimensional short-range order may start to already evolve at much higher temperatures. Here, we speculate that the

(24) Blinc, R.; Dolinšek, J.; Arčon, D.; Mihailovič, D.; Venturini, P. *Solid State Commun.* **1994**, *89*, 487.
(25) Tou, H.; Maniwa, Y.; Iwasa, Y.; Shimoda, H.; Mitani, T. *Phys. Rev. B: Condens. Matter Mater. Phys.* **2000**, *62*, 775.

fullerene···H−$CH_2NH_2$ interactions may play an important role in promoting a particular low-dimensional motif of Jahn−Teller statically deformed $C_{60}^{3-}$ ions.

The dipolar interactions between the unpaired $C_{60}^{3-}$ electron spins and the $^1$H nuclei are responsible for NMR spectral broadening. Using the results of the earlier $^2$H line shape analysis, we conclude that the observed increase in the $^1$H second moment, $\sqrt{M_2}$ at $T_S$ (Figure 4a) is also due to freezing out of the $CH_3NH_2$ molecular dynamics. We now focus on the additional $^1$H line shape broadening observed below $T_N$. This is caused by the electron−nuclear dipolar interaction between the antiferromagnetically ordered $C_{60}^{3-}$ moments and the $^1$H nuclei of the $CH_3NH_2$ molecule and depends sensitively on the type of long-range AFM ordering.[26] To calculate the $^1$H NMR line shape in the ordered state, we closely followed the formalism developed earlier by Tou et al. for ammoniated alkali fullerides.[26] In our calculations, we began by placing the $^1$H atoms in the crystallographic positions determined at room temperature for the orientationally disordered phase (i.e., the protons belonging to the $CH_3$ group are located at $\vec{\mathbf{r}}_H(CH_3) = (0.61099, 0.08350, 0.06836)$, while those of the $NH_2$ group at $\vec{\mathbf{r}}_H(NH_2) = (0.55758, 0.02934, 0))$.[4] We also assumed an effective magnetic moment per $C_{60}$ unit, $\mu_{eff} = 0.7\ \mu_B$, as determined before from antiferromagnetic resonance data,[6] and placed the unpaired electronic moments at the centers of the $C_{60}$ molecules. These moments produce a dipolar field at each $^1$H site given by

$$\vec{\mathbf{B}}_{loc}(\vec{\mathbf{r}}_H) = \frac{\mu_0}{4\pi}\sum_i \frac{1}{|\vec{\mathbf{r}}_i - \vec{\mathbf{r}}_H|^3}\left(3\frac{(\vec{\mu}_i(\vec{\mathbf{r}}_i - \vec{\mathbf{r}}_H))(\vec{\mathbf{r}}_i - \vec{\mathbf{r}}_H)}{|\vec{\mathbf{r}}_i - \vec{\mathbf{r}}_H|^2} - \vec{\mu}_i\right) \quad (3)$$

Here, the sum runs over all unpaired electrons at $\mathbf{r}_i$ sites with a $\mu_i$ moment aligned according to the specific type of antiferromagnetic order investigated. Since in our experiments the external magnetic field $B_0 = 6.3$ T is much larger than $B_{loc}$, only the component of $\vec{\mathbf{B}}_{loc}$ along $\vec{\mathbf{B}}_0$ determines the shift in the $^1$H resonance, $\delta\nu(\vartheta,\varphi) = \gamma_n \vec{\mathbf{B}}_{loc}\hat{\mathbf{n}}(\vartheta,\varphi)$, where $\hat{\mathbf{n}}(\vartheta,\varphi)$ is the unit vector defining the orientation of $\vec{\mathbf{B}}_0$ with respect to the unit cell and expressed in terms of polar and azimuthal angles $\vartheta$ and $\varphi$, respectively. To simulate the powder line shape, $\vartheta$ and $\varphi$ were randomly selected, and the complete NMR spectrum was obtained as a convolution of corresponding $CH_3$ and $NH_2$ resonances. The orientation of the individual magnetic moments $\vec{\mu}_i$ was obtained in the spin flop phase (spin flop field, $B_{sf} \approx 0.1$ T),[6] and four types of collinear AFM order were considered with ordering vectors $\vec{\mathbf{q}}_I = (0, 0, 1)$ (type I), $\vec{\mathbf{q}}_{II} = (1/2, 1/2, 1/2)$ (type II), $\vec{\mathbf{q}}_{III} = (1/2, 0, 0)$ (type III), and $\vec{\mathbf{q}}_{IV} = (1/2, 1/2, 0)$ (type IV) with respect to the face-centered orthorhombic unit cell. Best agreement between experimental and theoretical spectra was obtained for the collinear AFM type II structure where individual magnetic moments are aligned along the crystallographic $a$-axis and $\mu_1 = \mu_2 = -\mu_3 = \mu_4$ (Figure 7). We note that a similar magnetic structure was proposed for the related AFM $(NH_3)K_3C_{60}$ fulleride.[26] All other types of magnetic order investigated resulted in much broader line shapes that could not be reduced to the experimental line width under any reasonable assumptions. We note that the ordered magnetic moment per $C_{60}$ unit in $(CH_3NH_2)K_3C_{60}$ also was reduced below 1 $\mu_B$. This is reminiscent of the situation encountered before for both ferromagnetic (TDAE-$C_{60}$) and antiferromagnetic ($(NH_3)K_3C_{60}$) fullerides.[17,26,27] In analogy with these systems, we also anticipate that the degree of orbital order of the Jahn−Teller distorted $C_{60}^{3-}$ ions is responsible for the observed moment reduction.

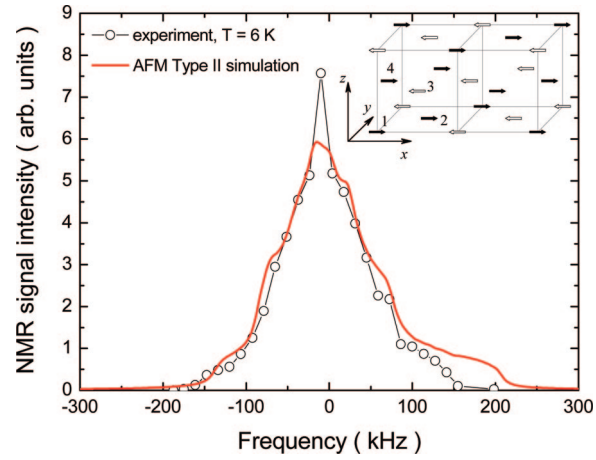


**Figure 7.** Comparison between experimental (at 6 K) and calculated $^1$H NMR spectra for AFM type II order in $(CH_3NH_2)K_3C_{60}$. Inset: proposed zero-field magnetic structure.

Finally, we briefly comment on the temperature dependence of the $^1$H spin lattice relaxation time, $T_1$, and its remarkable similarity to that of the X-band EPR line width (Figure 5). From the earlier discussion, we conclude that the electron−nuclear dipolar interaction is the dominant interaction present, and therefore, $T_1$ is principally determined by the $C_{60}$ unpaired electronic dipolar field fluctuations caused by flip-flops. In this case, the powder average expression for $T_1$ is given by[28,29]

$$\frac{1}{T_1} = \frac{2}{15}\left(\frac{\mu_0}{4\pi}\right)^2 \gamma_n^2 g^2 \mu_B^2 S(S+1)\sum_i r_i^{-6}\left(3\tau_e + \frac{7\tau_e}{1+\omega_S^2\tau_e^2}\right) \quad (4)$$

with the Larmor frequency of unpaired $C_{60}$ electrons at a distance $r_i$ from the $^1$H nuclei, $\omega_S = 1108$ GHz. The temperature dependence of the $^1$H spin lattice relaxation rate, $T_1^{-1}$ is therefore controlled by the electron spin correlation time, $\tau_e$. As in the present case $\omega_S\tau_e \gg 1$, eq 4 simplifies to $T_1^{-1} \propto \tau_e^{-1}$. The electronic correlations can decay via two relaxation channels[30]— either through the spin lattice coupling characterized by the electronic spin lattice relaxation time, $T_{1e}$, or through the spin flips of neighboring $C_{60}$ electronic moments characterized by the nearly temperature independent correlation time, $\tau_f$. As a result, we can write

(26) Blinc, R.; Jeglič, P.; Apih, T.; Seliger, J.; Arčon, D.; Dolinšek, J. *Phys. Rev. Lett.* **2002**, *88*, 86402.

(27) Simon, F.; Janossy, A.; Muranyi, F.; Feher, T.; Shimoda, H.; Iwasa, Y.; Forro, L. *Phys. Rev. B: Condens. Matter Mater. Phys.* **2000**, *61*, R3826.

(28) Noris, M. O.; Strange, J. H.; Powels, J. G.; Rhodes, M.; Marsed, K.; Krynicki, K. *J. Phys. C* **1968**, *1*, 422.

(29) Horiuchi, K.; Asaji, T.; Ikeda, R. *Phys. Rev. B: Condens. Matter Mater. Phys.* **1994**, *50*, 6169.

(30) Birkeland, A.; Svare, I. *Phys. Scr.* **1978**, *18*, 154.

$\tau_e^{-1} = T_{1e}^{-1} + \tau_f^{-1}$. However, the EPR line width is directly related to $T_{1e}$ by $\Delta H_{1/2} = 2/\gamma T_{1e}$, and therefore, it is not surprising that the temperature dependence of the $^1H$ spin lattice relaxation rate, $T_1^{-1}$, mimics that of the EPR line width, $\Delta H_{1/2}$ (inset to Figure 5).[5] The two curves begin to deviate from each other below ~70 K, precisely in the temperature range where spin correlations start to develop affecting the low-temperature relaxation.

## Conclusion

In conclusion, we measured the $^1H$ and $^2H$ NMR spectra of powdered $(CH_3NH_2)K_3C_{60}$ between room temperature and 4 K. The $^2H$ NMR line shape analysis revealed that the structural phase transition at $T_S = 220$ K, previously observed by synchrotron XRD,[4] is driven by the orientational ordering of the $K^+$-$ND_2CD_3$ units. The ordering transition is accompanied by a sudden increase in the hyperfine contact constant, $a_i$, providing the signature of a very small unpaired spin charge density transfer from the fulleride ions to the methylamine molecule of the $K^+$-$NH_2CH_3$ unit, indicative of the appearance of fullerene$\cdots$H$-$$CH_2NH_2$ interactions. Such interactions may be responsible for the development of spin correlations well above $T_N$ and the promotion of a particular order of statically Jahn$-$Teller distorted $C_{60}^{3-}$ units. Finally, the $^1H$ NMR spectra of $(CH_3NH_2)K_3C_{60}$ below $T_N = 11$ K are consistent with an ordered AFM structure of type II and a staggered moment per $C_{60}$ unit of ~0.7 $\mu_B$.

**Acknowledgment.** We thank the EPSRC for financial support (M.J.R. and K.P.).

CM800578E